

# Submicron-sized MoRe-doped Si-MoRe Josephson junctions with a low specific capacitance

A Kalenyuk<sup>1</sup>, A Shapovalov<sup>2</sup>, V Shnyrkov<sup>3</sup>, V Shaternik<sup>1</sup>, M Belogolovskii<sup>1,4</sup>, P Febvre<sup>5</sup>, F Schmidl<sup>6</sup> and P Seidel<sup>6</sup>

<sup>1</sup>G. V. Kurdyumov Institute for Metal Physics, National Academy of Sciences of Ukraine, Academician Vernadsky Blvd. 36, Kiev 03142, Ukraine

<sup>2</sup>V. N. Bakul Institute for Superhard Materials, Avtozavodskaya Str. 2, Kyiv 04074, Ukraine

<sup>3</sup>Kyiv Academic University, Academician Vernadsky Blvd. 36, Kiev 03142, Ukraine

<sup>4</sup>Vasyl' Stus Donetsk National University, 600-letiya Str. 21, Vinnytsia 21021, Ukraine

<sup>5</sup>Université Savoie Mont Blanc, Campus scientifique, Le Bourget du Lac cedex 73376, France

<sup>6</sup>Institut für Festkörperphysik, Friedrich-Schiller-Universität Jena, Helmholtzweg 5, Jena 07743, Germany

E-mail: paul.seidel@uni-jena.de

**Abstract.** We start with a short look at the problem of low-capacitance Josephson junctions, its history, and actual state-of-the-art. It is argued that such devices are important for applications requiring nonhysteretic current-voltage characteristics since reduction of capacitance by several times makes it possible to increase the device resistance by the same amount while keeping the McCumber-Stewart damping parameter unaltered. Moreover, at very high frequencies the capacitance in the RCSJ circuit with a parallel connection starts to shunt the superconducting current component due to reduction of the corresponding reactance inversely proportional to  $C$ . Hence, to extend the operating frequency range of a Josephson junction its capacitance should be as small as possible. As a solution of a new type of the Josephson device, less resistive and with smaller capacitance, we propose and realize a submicron-sized trilayer with tens nm-thick Si interlayer doped by metallic ultra-small inclusions and superconducting Mo-Re alloy electrodes.

## 1. Introduction

Conventional Josephson junction is made by sandwiching an ultra-thin layer of a non-superconducting material between two superconducting (S) electrodes possessing separate macroscopic wavefunctions, whose phase difference is  $\varphi$ . Although the fundamental nature of superconductivity and thus the junction dynamics is quantum in most cases the Josephson phase  $\varphi$  may be treated as a classical continuum variable, especially when the temperatures are not too low. Even more, if a pure quantum description is invoked it is necessary to prove that the results obtained indeed cannot be explained in



‘classical’ terms [1]. The actual “classical” way of modelling the Josephson systems dynamics is based on an equivalent circuit that captures the essential ingredients of a real Josephson setup. It consists of three parallel elements: a resistor  $R$ , a capacitor  $C$ , and a pure superconducting element with a certain supercurrent-versus-Josephson phase difference dependence  $I_c(\varphi)$ . Such approximation which proved its high efficiency is usually named ‘Resistively and Capacitively Shunted Junction’ (RCSJ) model [2].

In this paper, we are limiting ourselves to this approach since the experiments we are referring to were performed on conventional superconductors above 1.9 K, when the phase  $\varphi$  is not expected to take on attributes of a macroscopic quantum coordinate [1]. Within the RCSJ model, the Josephson-junction operation regime is controlled by the McCumber-Stewart damping parameter  $\beta_c$ , a product of the characteristic Josephson frequency  $\omega_c = 2eV_c / \hbar$ , where  $V_c = I_c R$ , and the decay time  $\tau = RC$  [3]

$$\beta_c = \frac{2eV_c RC}{\hbar}. \quad (1)$$

From the derivation of the  $\beta_c$  parameter it follows that nonhysteretic current-voltage ( $I - V$ ) characteristic is achieved when  $\beta_c$  is less than unity whereas for  $\beta_c > 1$  the  $I - V$  curve will be double-valued. In the subgap region  $eV < \Delta$  ( $\Delta$  is the superconducting energy gap), the resistance of a traditional SIS junction with a nm-thick insulating (I) interlayer is huge and, as a result,  $\beta_c \gg 1$ . The evident solution leading to single-valued behavior is to place an external low-resistance normal-metal shunt  $R_{sh} \ll R$  in parallel with the junction that reduces the total resistance  $R$  to values appropriate for  $\beta_c \sim 1$ . Unfortunately, such way results in a considerable complication of the circuitry design and introduces parasitic inductance through the junction.

Another possibility could be to diminish significantly the junction capacitance  $C$  but in SIS trilayers with an oxide barrier its value weakly depends on the interlayer modifications as it follows from the empirical formula connecting the specific capacitance  $c$  with the device normal-state resistivity  $\rho_N$   $c = (0.47 - 0.047 \log(\rho_N))^{-1}$  [pF/cm<sup>2</sup>] [4] valid for Nb-AlO<sub>x</sub>-Nb junctions, the most popular version of the SIS setups. The only possibility to suppress the total capacitance  $C$  is to shrink the SIS junction sizes but it will result in the growth of its resistance  $R$ . Therefore, it is necessary to look for alternative means of the  $C$  reduction to get rid of the hysteresis in the  $I - V$  curves. Another problem stimulating the search for low- $C$  Josephson devices is related to high-frequency applications when the capacitance in the RCSJ circuit with a parallel connection starts to shunt the superconducting current component due to reduction of the corresponding reactance inversely proportional to  $C$ . It is clear that to extend the operating frequency range of a Josephson junction its capacitance should be as small as possible and it should be done by the replacement of a conventional superconductor-insulator-superconductor device with a novel type of the trilayer, less resistive and with smaller capacitance.

In the next subsection, we argue that the problem of low capacitances cannot be solved within a traditional elemental base and analyze its solution based on doped semiconductors as non-superconducting interlayers. It is proposed to replace not only an I layer in the SIS junctions but also S electrodes with a Mo-Re alloy known by its mechanical durability and resistance to oxygen. In our opinion, the incorporation of these new materials into a single Josephson device can thoroughly improve its properties. The fourth subsection presents our experimental results obtained for submicron MoRe-doped Si-MoRe Josephson junctions and compare them with theoretical expectations. In Conclusions, we discuss perspectives of introducing the semiconductor-base Josephson setups into dc and rf SQUIDs.

## 2. Josephson junctions with a doped semiconductor as a weak link

To suppress the barrier resistance and simultaneously to diminish the junction capacitance is a complicated task. In order to solve it, we have to find a technologically acceptable material with a comparatively narrow gap between conduction and valence bands and a relatively low permittivity  $\varepsilon$  to

reduce the capacitance  $C$ . The first requirement is needed to get low and thick potential barrier for Cooper pairs and therefore low junction resistance  $R$  and capacitance  $C$ . The second one slightly contradicts the previous condition since the dielectric permittivity logarithmically decreases with the increase of the forbidden gap [5]. Hence, we should look for a compromise and an optimal material in this sense is a slightly doped silicon.

As is shown in the recent paper [6], in a doped Si-based barrier obtained by sputtering from a composite target (Si + W) metal nanoscale clusters with a characteristic size compared to the barrier thickness are formed in the silicon matrix due to the self-organization effect. The structural analysis [6] showed that, within this technology, both silicon and tungsten are in amorphous states. Thus, at small doping levels, the charge flow across the composed barrier will be locally dependent and occur through a large number of separate, actually one-dimensional paths than a uniform current across a device cross-section. Following this hypothesis, we suppose that the main part of the eigenchannels within the hybrid barrier has very low transmission coefficient  $D \ll 1$  while a very small portion of the interface is well transparent with  $D \leq 1$ . The latter ‘open’ channels, most probably, are distributed more or less uniformly in the form of filaments or resonance-percolating trajectories [7] having a diameter much less than the superconducting coherence length  $\xi_S$  in the junction electrodes whereas the distance between them exceeds  $\xi_S$ . In this case, the proximity effect on the S layers should be tiny and the superconducting order parameter, even near the NS interface, is untouched. The supercurrent that flows through the low-transparent (and thus tunnel-like) part of the weak link will follow the standard theory for SIS sandwiches while the transport of Cooper pairs across high-transparent eigenchannels, which realize internal shunting, is similar to Josephson trilayers with a normal-metal interlayer.

Previously [8] we argued that in strongly disordered conducting systems there can be a single governing dimensionless parameter  $Z$  controlling the channel conductance  $G$ . In general, the  $G(Z)$  dependence is sample-dependent but roughly can be described with a Lorentzian  $G(Z) = G_0/(1+Z^2)$  with the conductance quantum  $G_0 = 2e^2/h$ . Assume next that  $Z$  is a random variable uniformly distributed from zero to infinity, i.e., its probability density  $\rho(Z) = 2\hbar\bar{G}/e^2 = \text{const}$  with the disorder-averaged macroscopic conductance  $\bar{G}$  introduced to normalize  $\rho(Z)$ .

A large number of ‘open’ eigenchannels with the transparency  $D \leq 1$  would reveal themselves, in particular, in the emergence of an excess current  $I_{\text{exc}}$ , a constant shift of the superconducting  $I$ - $V$  curve towards that measured in the normal state at  $V$  exceeding  $\Delta/e$ . The ratio  $I_c/I_{\text{exc}}$  which has no fitting parameters can be calculated using the universal distribution function  $\rho(Z)$  and compared with the related quantity measured experimentally [8]. In the fourth subsection we follow this way for verifying our assumptions concerning a single controlling parameter  $Z$  and universality of the distribution function  $\rho(Z) = \text{const}$ . Using conventional relations for  $I_c$  and  $I_{\text{exc}}$  where the channel transparencies  $D(Z) = 1/(1+Z^2)$  and averaging over  $Z$  with  $\rho(Z)$  we obtain that  $I_c/I_{\text{exc}} \approx 1.7$  at zero temperature.

### 3. Mo-Re alloy electrodes for improved Josephson junctions

Superconducting electrodes made of Mo-Re alloys is the main difference of our Josephson samples from Nb-doped Si-Nb trilayers realized and studied in Refs. 9 and 10. Superconducting properties of the Mo-Re alloy were revealed during systematic studies of critical temperatures  $T_c$  in transition metals. In 70s it was found that the maximal  $T_c$  in bulk and film Mo-Re samples is reached in the A15 phase and can be as high as 15 K. It was found that the solubility of interstitial elements, in particular, of oxygen in the Mo-Re system is low and such contaminations do not depress superconductivity in a Mo-Re alloy [11]. The native oxide of the Mo-Re alloy is grown up to a thickness not more than 0.5 nm and are thinner than the oxides on Mo and Re surfaces, see the related discussion in Ref. 12. In order to form a low-leakage tunnel junction on the Mo-Re film, they had to cover it with an Al overlayer that was after that oxidized. Due to mechanical durability and resistance to oxygen, the Mo-Re system was proposed as a candidate for microwave cavities [11].

All reasons for practical applications of the Mo-Re alloy were summarized in Ref. 11. They are as follows: (i)  $T_c$  of a  $\text{Mo}_{1-x}\text{Re}_x$  film is usually higher than that of the bulk sample, whatever technique is used for its deposition; (ii) the maximum  $T_c \cong 15$  K reaches in a wide region of the composition for  $x$  ranging between 2.5 and 6.2 thanks to the presence of the A15 metastable phase; (iii) high deposition temperatures are necessary to achieve the maximal  $T_c$  value but  $T_c$ 's of above 11 K can be obtained by depositions performed at about 300 °C; (iv) Mo–Re alloys exhibit a low value of the Ginzburg-Landau parameter and consequently rather high critical field  $H_{c1}$  and coherence length, thus, they are not very sensitive to small imperfections. In the paper [12], using the literature data for lower and upper critical magnetic fields in the Mo-Re compound, the authors estimated the values of the coherence length  $\xi$  to be up to 100 nm. Recent study [13] of the full  $\text{Mo}_{1-x}\text{Re}_x$  binary phase diagram showed that critical temperatures of Mo-Re alloys form three different contiguous superconducting regions. Low-temperature electronic specific heat measurements in Ref. 13 revealed a fully-gapped superconducting state with a moderate electron-phonon pairing. The energy gap  $\Delta$  from tunneling measurements in the  $\text{Mo}_{0.6}\text{Re}_{0.4}$  compound [14] was found to be equal to 1.4 meV. The unique properties of this system have attracted an interest nowadays in order to create stable and well controlled superconducting heterostructures, see, for example, the fabrication of SQUID-on-tip nanodevices [15].

#### 4. Doped-silicon nanoscale interlayers for low-capacitance submicron-sized Josephson junctions

To form Si tunnel barriers with nanoscale W dopants, we used a target consisted of a pure Si wafer and a number of tungsten wires. The tungsten concentration  $c_W$  in the mixture was changed from 0 to 10 at %. Tens nanometer-thick Si(W) interlayers were deposited by DC sputtering at 0.1 Pa pressure in Ar flow. The transmission electron microscopy revealed the self-organized formation of tungsten implants inside the hybrid layer [6]. Whereas in ultra-thin Si(W) interlayers they formed nanoclusters, their typical size for a 10 nm-thick barrier was nearly its thickness. These results were confirmed by atomic force microscopy measurements and dependence of the nanoclusters formation on the tungsten content was explained by substantial difference between normal gradients of Van der Waals forces for metallic tungsten and the semiconductor matrix [6].

The first type of Josephson trilayers with the area of  $100 \times 100 \mu\text{m}^2$  was created using a traditional mask technology. It was found that the product of the critical current and the normal-state resistance  $V_c = I_c R_N$  for MoRe-Si(W)-MoRe junctions rises by increasing the rate of simultaneous deposition of Si(W) thin films. Typical  $V_c$  magnitudes as well as specific capacitance and resistance  $R_N$  values of the MoRe-Si(W)-MoRe junctions well agreed with results by Gudkov *et al* [9,10] for Nb/Si(W)/Nb junctions. However, we believe that the replacement of niobium, an active getter by the Mo-Re alloy leads to the increased stability of Josephson junctions.

The new type of submicron devices on sapphire substrates were fabricated by a combination of conventional optical lithography, metal deposition and additional focused ion beam (FIB) milling steps. At the first stage, a three-layered MoRe-Si(W)-MoRe structure was obtained by magnetron sputtering technique. After that pads and 5  $\mu\text{m}$ -wide stripes were patterned with the lithography and next we formed submicron-sized contacts by ion milling with the ion beam normal to the surface of the layered structure. At the last stage, the side cuts were made with the ion beam close to be parallel to the sample surface. Thus the intermediate layer of doped silicon, enclosed between two side cuts, played the role of the Josephson-junction barrier through which the supercurrent  $I_c$  was flowing. Figure 1 demonstrates a scanning-electron-microscopy (SEM) image of the obtained heterostructure as well as a side view of the Josephson junction formed by two Mo-Re electrodes with a doped-Si nanoscale barrier.

Current-voltage characteristics of such obtained junctions were measured over the temperature range from 1.9 to 9.0 K in zero applied magnetic field  $B = 0$  and at  $B = 70$  mT. A sample which has both a uniform junction barrier and current distribution should exhibit a Fraunhofer diffraction pattern for the regime when the Josephson penetration depth is larger than 1/4 of the junction width. Figure 2 shows an  $I_c$ -versus- $B$  curve for a representative sample at 6.5 K. The symmetry with respect to the central maximum indicates the sample homogeneity.

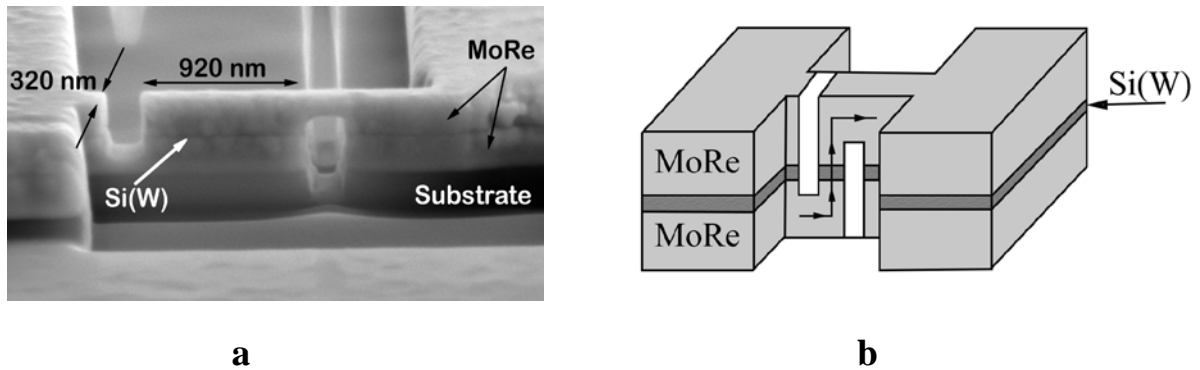


**Figure 1.** SEM micrograph of the heterostructure formed by a combination of optical lithography, metal deposition and FIB milling steps (a) and the schematic of the Josephson-junction side view where the internal arrow demonstrates the supercurrent flow direction (b)

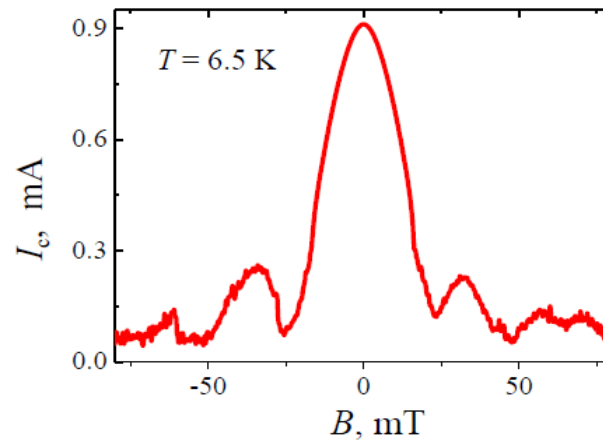


**Figure 2.** Magnetic-field effect on the critical current of a submicron-sized MoRe-Si(W)-MoRe Josephson junction at  $T = 6.5$  K

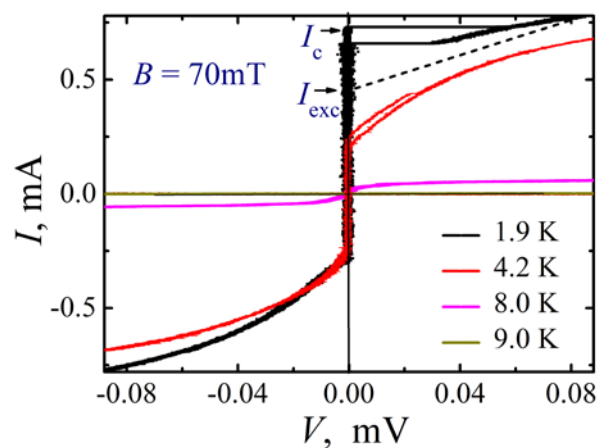


**Figure 3.** Temperature effect on the  $I$ - $V$  curves of a submicron-sized MoRe-Si(W)-MoRe Josephson junction in applied magnetic field  $B = 70$  mT,  $I_c$  is the critical current,  $I_{exc}$  is the excess current

Figure 3 demonstrates the temperature impact on the current-voltage characteristics for the same sample in the magnetic field of 70 mT. At 1.9 K, the lowest temperature of our experiments we can see a small hysteresis which disappears above 4.2 K. As follows from figure 2, the ratio  $I_c/I_{exc}$  at 1.9 K is equal to 1.56 in good agreement with the theoretical expectation.

### 5. dc & rf SQUIDS based on low-capacitance Josephson junctions

A promising field of the low-capacitance Josephson junction applications are dc and rf SQUIDS. Their operating principles are well described in the literature, thus in the following we discuss them only from the viewpoint of applying low-capacitance devices. The readout of macroscopic quantum states of a single superconducting qubit or a system of coupled qubits with the minimum back-action caused by the detector remains one of the most important engineering issues in quantum informatics. Reaching the quantum non-demolition limit is highly desirable for quantum computing. This limit is reached when the perturbation of the quantum state during the measurement does not go beyond that required by the measurement postulate of quantum mechanics, so repeated measurements of the same eigenstate lead to the same outcome. SQUID circuits can be integrated with superconducting qubits due to low dissipation, scalability, compatibility with the qubit fabrication process and their operation in a low temperature environment.

The dc SQUID consists of two Josephson SIS junctions with a critical current  $I_c$ , a capacitance  $C$  and a resistance  $R$  in a superconducting loop of the inductance  $L$ . The maximum zero-voltage current  $I_{max}$  that can be driven through the SQUID in the absence of an applied magnetic flux is  $2I_c$ . In order to eliminate hysteretic  $I$ - $V$  curves and dynamical noise, as was argued above, the McCumber-Stewart damping parameter  $\beta_c$  (1) should be less than unity. External shunt several-Ohm resistors reduce the voltage amplitude of the SQUID signal characteristics. Moreover, they can introduce intolerable back action (decoherence). Thus the noise generated by the shunting resistors should be sufficiently reduced and/or effectively decoupled from of the flux qubits or a single photon counter.

Numerical simulations in the classical limit [16] show that the white noise energy of dc SQUIDS has a minimum for  $\beta_c \cong 1$ , the characteristics inductance  $\beta_L = 2LI_c/\Phi_0 \cong 1$ , and the thermal noise parameter  $\Gamma = 2\pi k_B T / (\Phi_0 I_c) < 0.05$ ,  $\Phi_0$  is the quantum flux. To enhance dc SQUID performance, one should use Josephson junctions with the characteristic voltage  $I_c R$  as large as possible and at the same time with  $\beta_c \leq 1$  and  $\beta_L \approx 1$ . It can be realized using Josephson junctions with low specific capacitances since in this case we can increase values of the resistance  $R$  (hence, the transfer coefficient  $\eta \approx R/L$ ) and to decrease the flux noise power spectral density  $S_\phi \approx 16 k_B T L^2 / R$  by 3 - 4 times.

The rf SQUID is based on the ac Josephson effect and uses a single Josephson junction [16]. It is less sensitive compared to dc SQUID but is cheaper and easier to manufacture in smaller quantities. Application of low-capacitance Josephson junctions with high characteristic frequencies permits to increase the resistance and thus to decrease the characteristic time of the interferometer flux variation  $\sim L/R$  where  $L$  is the superconducting loop inductance. Such rf SQUIDS could improve measurements of magnetic flux variations from a single microwave photon counter in the ultra-high frequency regime.

### 6. Conclusions

In the present work, we intended to draw attention to the problem of low-capacitance Josephson junctions. For implementations requiring non-hysteretic setups decrease in capacitance by several times makes it possible to increase the device resistance by the same amount while keeping the McCumber-Stewart damping parameter unaltered. In dc SQUIDS it allows to increase the transfer coefficient and to reduce the flux noise power spectral density as well as to decrease the response time in rf SQUIDS.

The best solution, in our opinion, would be an internally shunted Josephson junction with a comparatively thick hybrid barrier and, as a result, with low capacitance. The device satisfying these conditions is a trilayer with tens nm-thick semiconducting interlayer doped by metallic ultra-small

inclusions. As superconducting electrodes, we have proposed Mo-Re alloy layers with nearly equal concentrations of constituent elements. Their critical temperature is about 10 K (Fig. 2), the films are mechanically resistant and do not oxidize so actively as those of niobium. We can expect that such Josephson junctions will find new promising applications in superconducting electronics.

### Acknowledgements

A.K. and V.Sh. are grateful to the support from the Targeted Research & Development Initiatives Programme funded by the STCU and the National Academy of Science of Ukraine (Project No. 6250). P.S. is thankful to the support from the joint German-Ukrainian project “Controllable quantum-information transfer in superconducting networks” (DFG project number SE 664/21). The work was partly performed within a joint French-Ukrainian project supported by the French-Ukrainian Partenariat Hubert Curien (Project DNIPRO No. 37984RL) and the Ministry for Education and Science (MES) of Ukraine (Project M-62/2019). The authors are thankful to T. Golod and V. M. Krasnov for 3D FIB nano-sculpturing of the samples.

### References

- [1] Blackburn J A, Cirillo M and Grønbech-Jensen N 2016 *Phys. Rep.* **611** 1
- [2] Braginski A I 2019 *J. Supercond. Nov. Magn.* **32** 23
- [3] Lacquaniti V, Andreone D, De Leo N, Fretto M, Sosso A and Belogolovskii M 2009 *IEEE Trans. Appl. Supercond.* **19** 234
- [4] Yamamoto T, Suzuki S, Takahashi K, Yoshisato Y and Maekawa S 1995 *Appl. Phys. Lett.* **66** 1000
- [5] Sheka D I and Kokol A N 1976 *phys. stat. sol. (b)* **76** 413
- [6] Shapovalov A P, Shaternik V E, Turutanov O G, Lyakhno V Yu and Shnyrkov V I 2019 *Low Temp. Phys.* **45**, 776
- [7] Belogolovskii M, Zhitlukhina E, Lacquaniti V, De Leo N, Fretto M and Sosso A 2017 *Low Temp. Phys.* **43**, 756
- [8] Lacquaniti V, Cassiagio C, De Leo N, Fretto M, Sosso A, Febvre P, Shaternik V, Shapovalov A, Suvorov O, Belogolovskii M and Seidel P 2016 *IEEE Trans. Appl. Supercond.* **26**, 1100505
- [9] Gudkov A L, Kupriyanov M Yu and Likharev K K 1988 *Sov. Phys. JETP* **67**, 1478
- [10] Gudkov A L, Kupriyanov M Yu and Samus' A N 2012 *JETP* **114**, 818
- [11] Deambrosis S M, Keppel G, Ramazzo V, Roncolato C, Sharma R G and Palmieri V 2006 *Physica C* **441**, 108-113
- [12] Rudenko E, Solomakha D, Korotash I, Febvre P, Zhitlukhina E and Belogolovskii M 2017 *IEEE Trans. Appl. Supercond.* **27** 1800105
- [13] Shang T, Gawryluk D J, Verezhak J A T, Pomjakushina E, Shi M, Medarde M, Mesot J and Shiroka T 2019 *Phys. Rev. Materials* **3** 024801
- [14] Talvacchio J, Janocko M A and Gregg J 1986 *J. Low Temp. Phys.* **64**, 395
- [15] Bagani K, Sarkar J, Uri A, Rappaport M L, Huber M E, Zeldov E and Myasoedov Yu 2019 Sputtered MoRe SQUID-on-tip for high-field magnetic and thermal nanoimaging *Preprint cond-mat/1908.09305*
- [16] Fagaly R L 2015 *Applied Superconductivity. Handbook on Devices and Applications* vol 2, ed P Seidel (Weinheim: Wiley-VCH) pp 952-966